

Multiband Microstrip Patch Antenna for Communication and Navigation Applications

Xiao Fan¹⁺, Yandi Huang¹, Song Shi¹, Xiaoyu Wang¹, Xin Wang¹, Nan Mei¹, Jin Liu¹, and Hui Gao¹

¹ Institute of Urban Safety and Environmental Science, Beijing Academy of Science and Technology, Beijing 100054, China

Abstract. With the rapid development of satellite communication, satellite navigation, and wireless communication systems, multiband antennas are widely studied for military and commercial applications. To cover multiple frequency bands, we designed a multiband and wideband microstrip patch antenna with four multiple concentric rings fabricated on upper layer. Meander, fractals, and feeders covered with magnetic material could be beneficial to achieving relatively lower frequency bands. The novel layout optimizes the space utilization of the antenna and excites at multiple resonant modes. As a result, the proposed structure could obtain 7 operating bands of 0.35-0.57 GHz, 0.81-1.10 GHz, 1.2-2.0 GHz, 2.14-2.51 GHz, 2.63-2.70 GHz, 2.75-3.55 GHz, and 3.82-6.97 GHz and cover 21 popular bands for S-Band and C-Band satellite communications, the second generation BDS, GPS, and 2G, 3G, 4G, 5G, WiFi, WiMAX, WLAN, WMT, and HAPS wireless communication systems. This antenna could be widely used in multi-frequency satellite communication, satellite navigation, and wireless communication systems and our results provide support for further research on miniaturized ultra-multiband antennas.

Keywords: antenna design, modeling and measurements, computer aided design

1. Introduction

Due to the rapid development of satellite communication, satellite navigation, and wireless communication and the gradual increase of frequency bands, it is of great significance to realize multi-band and high-performance antenna in a smaller size. The multiband and wideband of the antenna directly determine the integration, performance, and complexity of the communication and navigation devices, which could cover more frequency bands simultaneously and reduce the number of antennas used. In the communication device, an antenna needs to cover the popular services including 2G, 3G, and 4G bands, such as GSM850 (824-894 MHz), GSM900 (880-960 MHz), DCS1800 (1710-1880 MHz), PCS1900 (1850-1990 MHz), LTE850 (869-894 MHz), LTE2190/2000S (2.18-2.20 GHz), LTE5537.5 (5.150-5.925 GHz), and 4.8 GHz (4.6-5.0 GHz) bands for 5G system. Apart from that, narrowband services including IEEE 802.11ah (0.9 GHz) and 802.11ac (5.8 GHz) bands for WiFi, WiMAX (3.40-3.65 GHz and 5.25-5.85 GHz), WLAN (5.15-5.35 GHz, 5.470-5.725 GHz, and 5.725-5.875 GHz), Wireless Medical Telemetry (WMT, 1.41-1.45 GHz), and High Altitude Platform Stations (HAPS, 6.44-6.64 GHz) should be covered. For Global Navigation Satellite System (GNSS), satellite navigation bands including B1 (1.559-1.592 GHz), B3 (1.251-1.286 GHz), and L (1.610-1.626 GHz) bands for the second generation Beidou Navigation Satellite system (BDS), L1 (1575.42±1.023 MHz), L2 (1227.6±1.023 MHz), and L5 (1176.45±1.023 MHz) bands for Global Positioning System (GPS), and so on should be covered.

The multiband and wideband of the antenna are key issue to keep good performance of the device. Diverse techniques, such as proximity coupling, meander, fractals, and so on, play important roles in exciting the multiple resonance modes, enhancing the bandwidth, and extending to relatively lower bands for patch antenna [1]. Recently, many multiband and wideband patch antennas have been reported in the literature [2-14]. A half-loop frame antenna with an overall dimension of 150.8×200.8×7 mm³ achieved dual operating bands of 746-960 MHz and 1710-2690 MHz for LTE metal-casing tablet device [15]. An octa-band

⁺ Corresponding author.
E-mail address: fanxiao@bmilp.com.

monopole antenna with a lumped-element high-pass matching circuit attained dual impedance bands of 0.69-0.98 GHz and 1.63-2.74 GHz [16]. The antenna consists of a V-slot loaded patch proximity coupled by an L-shaped feed resulting operating bands of 2.40-2.48 GHz, 3.44-3.53 GHz, 3.8-4.2 GHz, and 4.74-6.00 GHz for WiFi, WiMAX, and WLAN [1]. The antenna is comprised of a monopole with four branches and a dual-branch ground strip with an overall size of $75 \times 140 \times 5.8 \text{ mm}^3$. The antenna could achieve 5 operating bands of 681-991 MHz, 1626-2706 MHz, 3300-3813 MHz, 5136-5379 MHz, and 5622-6000 MHz, which could operate over LTE700, GSM850, GSM900, DCS, PCS, UMTS, LTE2300, LTE2500, and LTE3400 for 2G, 3G, and 4G systems, 3.5 GHz for WiMAX, and 5.2 GHz and 5.8 GHz for WLAN bands, but the WMT, WiFi5.5, and 5G bands are not covered [17]. It is hard to design antenna with multiband and wideband from 0.3 GHz to 7.0 GHz including UHF (0.3-3.0 GHz), L band (1-2 GHz), S band (2-4 GHz), and C band (4-8 GHz). To our best knowledge, very few antennas have been reported that could cover 21 popular bands including B1, B3, and L bands for the second generation BDS, L1 and L2 bands for GPS, GSM850, GSM900, DCS1800, PCS1900, LTE850, LTE2190/2000S, and LTE5537.5 bands for 2G, 3G, and 4G systems, 4.8 GHz for 5G system, IEEE 802.11ah and 802.11ac for WiFi, 1.41-1.45 GHz for WMT, 5.25-5.85 GHz for WiMAX, 5.15-5.35 GHz, 5.470-5.725 GHz, and 5.725-5.875 GHz for WLAN, and 6.44-6.64 GHz for HAPS. Moreover, a large number of antennas use lumped elements to match the circuit or use double-sided production, which increase the manufacturing cost and complexity.

In this paper, we get a multiband and wideband patch antenna, which consists of multiple concentric rings with parasitic element to create multiband. Meander, fractals, and magnetic cuboids covering feeders play vital roles in downshift of the frequency bands. The proposed antenna could achieve 7 operating bands of 0.35-0.57 GHz, 0.81-1.10 GHz, 1.2-2.0 GHz, 2.14-2.51 GHz, 2.63-2.70 GHz, 2.75-3.55 GHz, and 3.82-6.97 GHz and cover 21 popular bands in UHF, L, S, and C bands. The antenna could be applied to S- and C-Band satellite communications, the second generation BDS, GPS, and 2G, 3G, 4G, 5G, WiFi, WiMAX, WLAN, WMT, and HAPS wireless communication systems.

2. Design Structure

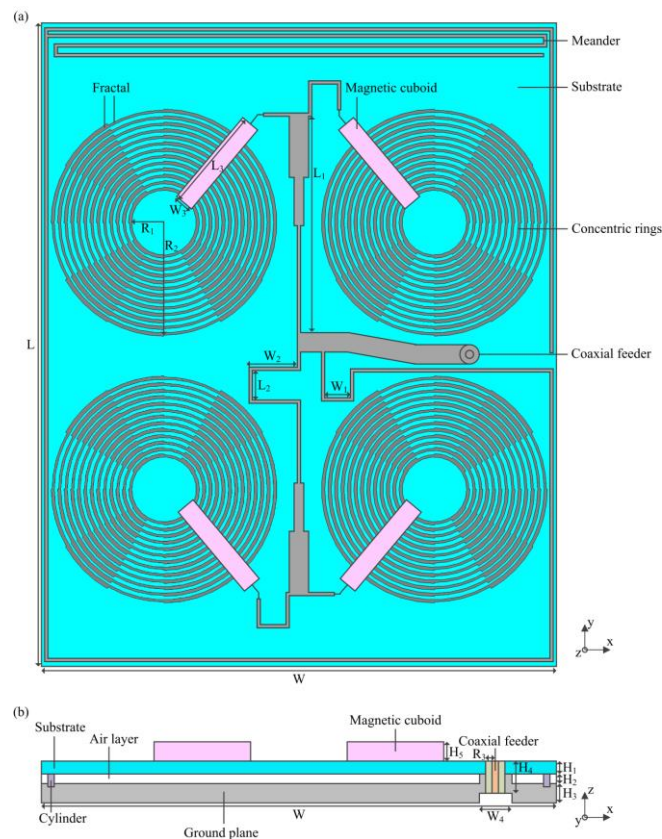


Fig. 1: The configuration of the proposed patch antenna with $L = 200 \text{ mm}$, $L_1 = 66.4 \text{ mm}$, $L_2 = 11.2 \text{ mm}$, $L_3 = 32 \text{ mm}$, $W = 160 \text{ mm}$, $W_1 = 8 \text{ mm}$, $W_2 = 16 \text{ mm}$, $W_3 = 6 \text{ mm}$, $W_4 = 10 \text{ mm}$, $H_1 = 4 \text{ mm}$, $H_2 = 3 \text{ mm}$, $H_3 = 6 \text{ mm}$, $H_4 = 10 \text{ mm}$, $H_5 = 6 \text{ mm}$, $R_1 = 10 \text{ mm}$, $R_2 = 35 \text{ mm}$, and $R_3 = 2.9 \text{ mm}$. (a) Top view. (b) Side view.

The structure of the proposed patch antenna is shown in Fig. 1, and the size of the antenna is $160 \times 200 \times 19 \text{ mm}^3$. The structure mainly consists of a rectangular patch antenna on one side of high dielectric permittivity substrate and metal ground plane on the other side. To reduce the quality factor Q value and expand the impedance bandwidth, the air layer is added between the substrate and metal ground plane except near the probe of the coaxial feeder to avoid inductance, as shown in Fig. 1(b). The cylinders with Teflon_Based material ($\epsilon = 2.08$) are placed on the four corners of the ground plane to support the substrate. The upper layer is composed of four two-dimensional metallic multiple concentric rings with fractal to excite preferred multiple resonance modes, which are in mirror symmetric manner, as shown in Fig. 1(a). The metallic meander is printed on the edge of the upper layer. The branch concentric rings and branch meander are connected to the five-branch feed line with 50Ω characteristics impedance. Specifically, the concentric rings are connected to the feed line through a microstrip line covered by the magnetic cuboid ($\epsilon = 11.4$, $\tan\delta = 0.19$, $\mu = 4.9$, $\tan\mu = 0.31$, $6 \times 32 \times 6 \text{ mm}^3$).

The simulation is performed using CST studio suite 2015.

3. Result and Discussion

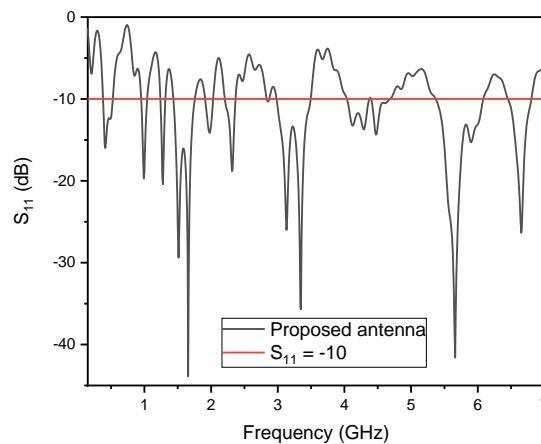


Fig. 2: The reflection coefficient of the proposed antenna.

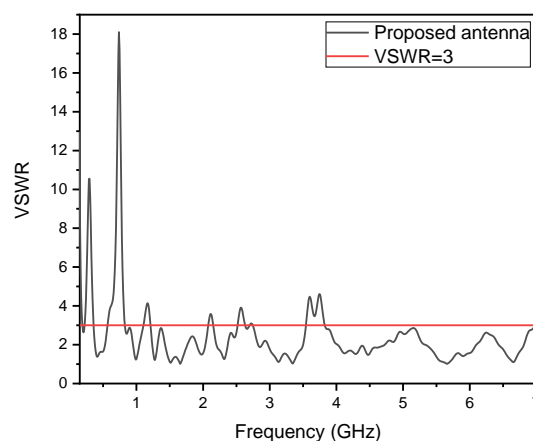


Fig. 3: The VSWR of the proposed antenna.

Fig. 2 illustrates the reflection (S_{11}) coefficient of the proposed patch antenna. The -10 dB impedance bandwidths are obtained at 0.38-0.52 GHz, 0.94-1.04 GHz, 1.24-1.31 GHz, 1.43-1.75 GHz, 1.91-2.03 GHz, 2.20-2.37 GHz, 2.98-3.49 GHz, 4.03-4.69 GHz, 5.37-6.08 GHz, and 6.44-6.80 GHz, respectively. As shown in Fig. 3, the Voltage Standing Wave Ratio (VSWR, reference 3) is observed at 0.35-0.57 GHz, 0.81-1.10

GHz, 1.2-2.0 GHz, 2.14-2.51 GHz, 2.63-2.70 GHz, 2.75-3.55 GHz, and 3.82-6.97 GHz and relative bandwidths reach 47.8%, 30.4%, 50.0%, 15.9%, 2.6%, 25.4%, and 58.4%, respectively. S_{11} and VSWR could characterize the signal reflection and operating frequency of the antenna. Combining the simulated results of S_{11} and VSWR, wide impedance bandwidths are obtained at the resonance frequencies 0.42 GHz, 0.99 GHz, 1.29 GHz, 1.50 GHz, 1.63 GHz, 1.98 GHz, 2.32 GHz, 3.12 GHz, 3.33 GHz, 4.13 GHz, 4.29 GHz, 4.49 GHz, 5.60 GHz, 5.98 GHz, and 6.66 GHz. The results indicate that the antenna attains 7 impedance bands of 0.35-0.57 GHz, 0.81-1.10 GHz, 1.2-2.0 GHz, 2.14-2.51 GHz, 2.63-2.70 GHz, 2.75-3.55 GHz, and 3.82-6.97 GHz, which could operate 21 popular bands for satellite communication, satellite navigation, wireless communication, and radar systems in UHF, L, S, and C bands. The frequency range of 0.35-0.57 GHz, 0.81-1.10 GHz, and 1.2-2.0 GHz in UHF and L-band could be used in B1, B3, and L bands for the second generation BDS, L1 and L2 bands for GPS, GSM850, GSM900, DCS1800, PCS1900, LTE850, IEEE 802.11ah for WiFi, and WMT. The achieved S-band (2.14-2.51 GHz, 2.63-2.70 GHz, 2.75-3.55 GHz, and 3.82-4.00 GHz) could have applications in LTE2190/2000S, mobile satellite communications, and weather ship radar. The achieved C-band (4.00-6.97 GHz) could be used in LTE5537.5, the 4.8 GHz for 5G, IEEE 802.11ac for WiFi, WiMAX, WLAN, HAPS, satellite communication, and weather radar system. In addition to popular bands, achieved bands (3.82-4.20 GHz) may be used for fixed satellite communication.

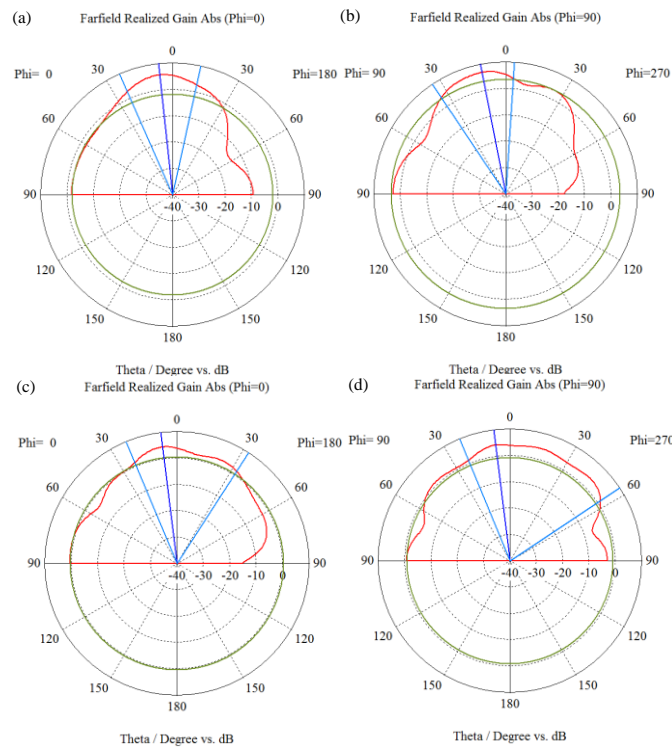


Fig. 4: The simulated far-field-patterns of the proposed antenna. (a) E-plane at 4.29 GHz. (b) H-plane at 4.29 GHz. (c) E-plane at 5.60 GHz. (d) H-plane at 5.60 GHz.

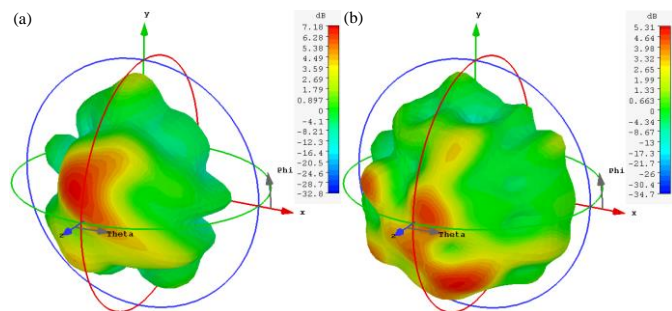


Fig. 5: The simulated three-dimensional far-field-patterns of the proposed antenna. (a) 4.29 GHz. (b) 5.60 GHz.

To get the radiation characteristics of the proposed antenna, the simulated far-field-patterns (E-plane, H-plane) are calculated at 4.29 GHz and 5.60 GHz with relatively lower VSWR values, respectively. The 3 dB angular widths at 4.29 GHz are 36 ° and 37.5 ° for the E-plane and H-plane radiation patterns, respectively, as shown in Fig. 4(a) and Fig. 4(b). The 3 dB angular widths at 5.60 GHz are 55.5 ° and 78.8 ° for the E-plane and H-plane radiation patterns, respectively, as shown in Fig. 4(c) and Fig. 4(d). At 4.29 GHz, the radiation gain 6.87 dB occurs at 11 ° as shown in Fig. 4(b). At 5.60 GHz, the radiation gain 4.48 dB occurs at 7 ° as shown in Fig. 4(c). The simulated three-dimensional far-field-patterns are displayed in Fig. 5. The radiation gain at 4.29 GHz is 7.18 dB as shown in Fig. 5(a), whereas the radiation gain at 5.60 GHz is 5.31 dB as depicted in Fig. 5(b). It indicates that the antenna has good performance in radiation gain and 3 dB angular width at C-band, making it suitable to apply in satellite communication, satellite navigation, and wireless communication.

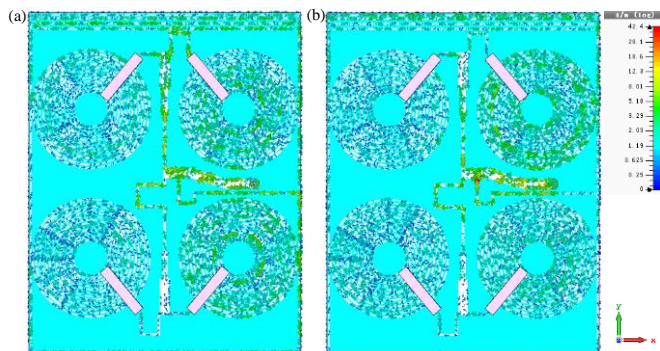


Fig. 6: The surface current distribution of the proposed antenna. (a) 4.29 GHz. (b) 5.60 GHz.

The operating mechanism of the proposed patch antenna is further explained using the surface current distribution. The surface current distribution is presented at 4.29 GHz and 5.60 GHz, respectively, as shown in Fig. 6. The surface current is highly concentrated at the feeders, multiple concentric rings, and meander, indicating that the radiation is mainly generated by them. The multiple concentric rings with proximity coupling can form a multi-resonant structure, making the antenna enhance bandwidth and excite preferred multiple resonance modes with impedance matching. The meander and fractals can significantly increase the current flow path and provide longer electrical length, which are of benefit to the downshift of the frequency bands. The magnetic cuboid covering feeders with strong radiation could be conducive to the miniaturization of antenna by shortening the wavelength that enters the magnetic cuboid. By adjusting the structure and parameters of the antenna, the antenna could achieve desired multiple operating frequency bands, improve the performance while reducing the size as much as possible.

The size and performance of the proposed antenna compared with other multiband antennas of current researches are listed in TABLE I. The proposed antenna has a significant advantage in the multi-band operation. None of the antennas reported in the literature [9] [15] [18-20] could cover as many popular bands as the proposed antenna does. Besides, there are no lumped element and double-sided production in the antenna, making it easier to use with low fabrication cost and complexity. Therefore, the advantages of the proposed antenna, such as more operating bands and lower fabrication cost and complexity, make it suitable for working in S- and C-Band satellite communications, the second generation BDS, GPS, and 2G, 3G, 4G, 5G, WiFi, WiMAX, WLAN, WMT, and HAPS wireless communication systems.

Table 1: Comparison of proposed antenna and references

References	Overall size (mm ³)	Operating bands (Relative bandwidth)	Used lumped elements
[9]	79×142×7.5	0.67-0.97 GHz (36.6%)	Yes
		1.61-2.80 GHz (54.0%)	
[15]	150.8×200.8×7	0.75-0.96 GHz (24.6%)	Yes
		1.71-2.69 GHz	

		(44.5%)	
[18]	280×280×20	0.69-0.96 GHz (32.9%)	No
		3.5-4.9 GHz (33.3%)	
[19]	115×102×45	0.80-0.98 GHz (20.2%)	No
		1.54-2.86 GHz (60.0%)	
[20]	75×140×5.8	0.70-0.96 GHz (31.3%)	Yes
		1.71-2.69 GHz (44.5%)	
		3.40-3.80 GHz (11.1%)	
This work	160×200×19	0.35-0.57 GHz (47.8%)	No
		0.81-1.10 GHz (30.4%)	
		1.2-2.0 GHz (50.0%)	
		2.14-2.51 GHz (15.9%)	
		2.63-2.70 GHz (2.6%)	
		2.75-3.55 GHz (25.4%)	
		3.82-6.97 GHz (58.4%)	

4. Conclusion

We proposed a multiband and wideband microstrip patch antenna. The antenna mainly consists of multiple concentric rings with fractals, feeders covered with magnetic material, and meander, resulting preferred multiple resonance modes and 7 operating bands. The radiation gain at 4.29 GHz and 5.60 GHz are 6.87 dB and 4.48 dB, respectively. The proposed antenna could cover 21 popular bands in S- and C-Band satellite communications, the second generation BDS, GPS, and 2G, 3G, 4G, 5G, WiFi, WiMAX, WLAN, WMT, and HAPS wireless communication systems without any lumped elements and double-sided production. The results indicate that the proposed patch antenna is a good candidate for applications in satellite communication, satellite navigation, and wireless communication systems.

5. Acknowledgements

This work was supported by the Innovation Cultivation Project of Institute of Urban Safety and Environmental Science, Beijing Academy of Science and Technology (Grant No. K139), the Reform and Development Project of Beijing Municipal Institute of Labor Protection (Grant No. K120-15), and the Backbone Individual Project of Excellent Talent Training and Funding of Xicheng District of Beijing.

6. References

- [1] R. Varma, and J. Ghosh. Multi-band proximity coupled microstrip antenna for wireless applications. *Microw. Opt. Technol. Lett.* 2018, **60**: 424-428.
- [2] C. Chiu, and W. Chuang. A novel dual-band spiral antenna for a satellite and terrestrial communication system. *IEEE Antennas Wirel. Propag. Lett.* 2009, **8**: 624-626.
- [3] K. F. Lee, S. L. S. Yang, and A. Kishk. The versatile U-slot patch antenna. *2009 3rd European Conference on Antennas and Propagation.* 2009.

- [4] Y. Chen, Y. Jiao, and G. Zhao. Dual-band dual-sense circularly polarized slot antenna with a C-shaped grounded strip. *IEEE Antennas Wirel. Propag. Lett.* 2011, **10**: 915-918.
- [5] L. Zheng, and S. Gao. Compact dual-band printed square quadrifilar helix antenna for global navigation satellite system receivers. *Microw. Opt. Technol. Lett.* 2011, **53**: 993-997.
- [6] W. C. Mok, S. H. Wong, and K. M. Luk. Single-layer single-patch dual-band and triple-band patch antennas. *IEEE Trans. Antennas Propag.* 2013, **61**: 4341-4344.
- [7] V. Singh, B. Mishra, and P. Narayan Tripathi. A compact quad-band microstrip antenna for S and C-band applications. *Microw. Opt. Technol. Lett.* 2016, **58**: 1365-1369.
- [8] D. Huang, and Z. Du. Eight-band antenna with a small ground clearance for LTE metal-frame mobile phone applications. *IEEE Antennas Wirel. Propag. Lett.* 2018, **17**: 34-37.
- [9] D. Huang, Z. Du, and Y. Wang. Eight-band antenna for full-screen metal frame LTE mobile phones. *IEEE Trans. Antennas Propag.* 2019, **67**: 1527-1534.
- [10] A. Affandi, R. Azim, and M. M. Alam. A low-profile wideband antenna for WWAN/LTE applications. *Electronics.* 2020, **9**: 393.
- [11] D. Huang, Z. Du, and Y. Wang. Compact thirteen-band antenna for 4G/5G/WLAN metal frame mobile phones. *INT J RF MICROW C E.* 2020, **30**: e22057.
- [12] R. Azim, T. Alam, and M. S. Mia. An octa-band planar monopole antenna for portable communication devices. *Sci. Rep.* 2021, **11**: 15298.
- [13] M. M. Hassan, M. Hussain, and A. A. Khan. Dual-band B-shaped antenna array for satellite applications. *INT J MICROW WIREL T.* 2021, **13**: 851-858.
- [14] K. C. Rao, P. M. Rao, and M. L. Naidu. A compact rectangular dual patch antenna for multiple satellite communication applications. *Wirel. Pers. Commun.* 2021, **122**: 1007-1041.
- [15] K. L. Wong, C. Y. Tsai. Half-loop frame antenna for the LTE metal-casing tablet device. *IEEE Trans. Antennas Propag.* 2017, **65**: 71-81.
- [16] Y. Wang, and Z. W. Du. Wideband monopole antenna with less nonground portion for octa-band WWAN/LTE mobile phones. *IEEE Trans. Antennas Propag.* 2016, **64**: 383-388.
- [17] Z. Eskandari, A. Keshtkar, and J. Ahmadi-Shokouh. A narrow-frame antenna for WWAN/LTE/WiMAX/WLAN mobile phones. *Int J Electron Commun.* 2018, **94**: 244-252.
- [18] Y. K. Chen, J. C. Zhao, and S. W. Yang. A novel stacked antenna configuration and its applications in dual-band shared-aperture base station antenna array designs. *IEEE Trans. Antennas Propag.* 2019, **67**: 7234-7241.
- [19] Y. H. Cui, R. L. Li, and P. Wang. Novel dual-broadband planar antenna and its array for 2G/3G/LTE base stations. *IEEE Trans. Antennas Propag.* 2013, **61**: 1132-1139.
- [20] K. L. Wong, and Y. C. Chen. Small-size hybrid loop/open-slot antenna for the LTE smartphone. *IEEE Trans. Antennas Propag.* 2015, **63**: 5837-5841.